associated with negative values of term III. Such conditions are present in the SBL at night over land, or anytime the surface is colder than the overlying air. An example of the decay of turbulence in negatively buoyant conditions just after sunset is shown in the budget profiles of Fig 5.6.

This same type of consumption can occur at the top of a ML, where warmer air entrained downward by turbulence opposes the descent because of its buoyancy (Stage and Businger, 1981). This is related to the negative values of the buoyancy term near the top of the ML in Fig 5.4.

5.2.4 Term IV: Mechanical (Shear) Production

When there is a turbulent momentum flux in the presence of a mean wind shear, the interaction between the two tends to generate more turbulence. Even though a negative sign precedes Term IV, the momentum flux is usually of opposite sign from the mean shear, resulting in production, not loss, of turbulence.

Fig. 5.4 shows case studies of the contribution of shear production to the TKE budget for convective situations. The greatest wind shear magnitude occurs at the surface. Not surprisingly, the maximum shear production rate also occurs there. As shown in Chapters 1 and 3, the wind speed frequently varies little with height in the ML above the surface layer, resulting in near zero shear and near zero shear production of turbulence. Shear production is often associated with the surface layer because of its limited vertical extent.

A smaller maximum of shear production sometimes occurs at the top of the ML because of the wind shear across the entrainment zone. In that region, the subgeostrophic winds of the ML recover to their geostrophic values above the ML.

The relative contributions of the buoyancy and shear terms can be used to classify the nature of convection (see Fig 5.7) ***Free convection*** scaling is valid when the buoyancy term is much larger than the mechanical term, ***forced convection*** scaling is valid when the opposite is true.

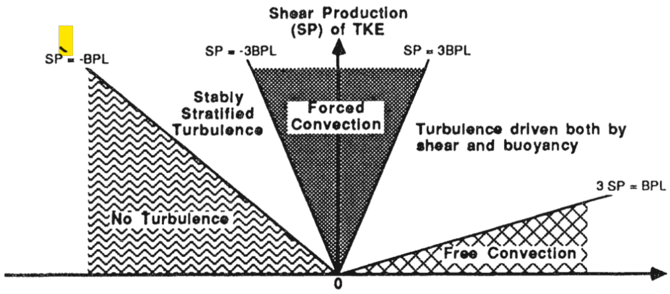

Fig. 5.7 Approximate regimes of free and forced convection.

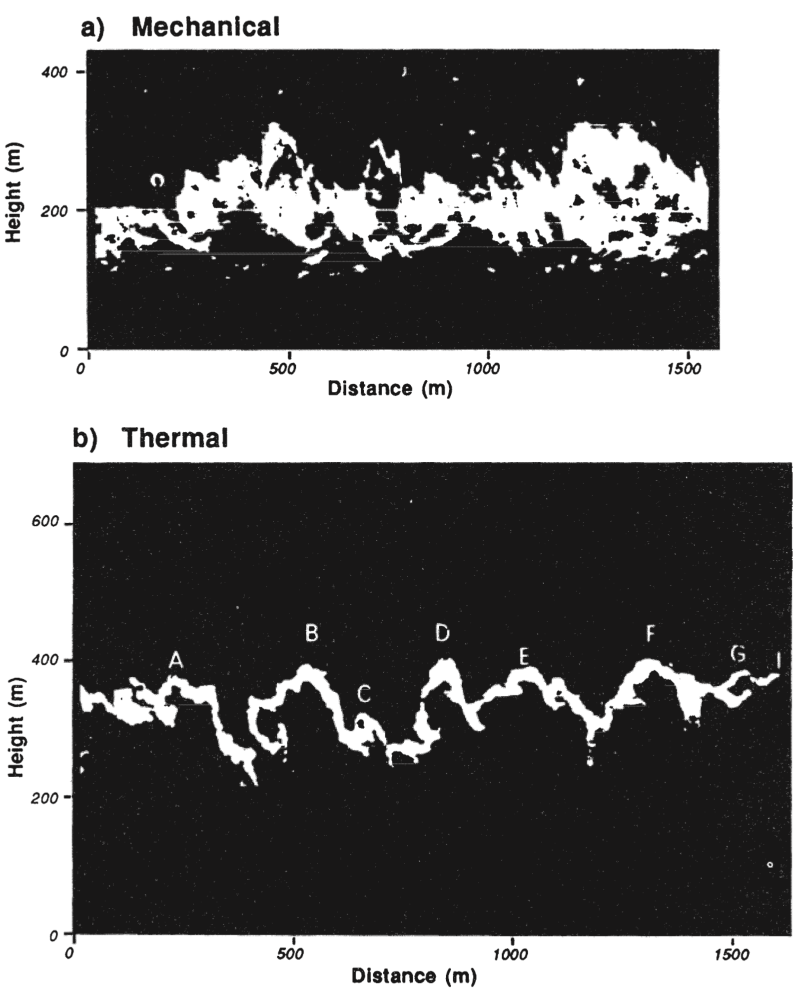

Fig. 5.8 Radar images of turbulence near the boundary layer top, showing (a) forced convection, and (b) free convection. After Noonkester (1974).

Magnitudes of the shear production term in the surface layer are obviously greatest on a windy day, and are small on a calm day. In synoptic-scale cyclones the strong winds and overcast skies suggest that forced convection is applicable. On many days, turbulence is neither in a state of free nor forced convection because both the shear and buoyancy terms are contributing to the production of turbulence.

At night over land, or anytime the ground is colder than the air, the shear term is often the only term that generates turbulence. We have seen from Fig 5.4 that the shear term is active over just a relatively small depth of air, so it is not surprising that, over land, the NBL is usually thinner than the ML.

The greatest shears are associated with the change of U and V components of mean wind with height. Except in thunderstorms, shear of W is negligible in the BL. Looking back on (4.3.1h-j), the shear production is greatest into the x and y components of TKE. Hence, shear production is also an anisotropic forcing — strongest in the horizontal.

Both the buoyant and shear production terms can generate anisotropic turbulence. The difference is that shear generation produces turbulence primarily in the horizontal directions, while buoyant generation produces it primarily in the vertical. These differences are evident in Fig. 5.8, where a high powered vertically pointing continuous-wave radar was used to observed the time evolution of eddy structure within the BL. This instrument senses moisture contrasts between dry and moist air. The boundary between regions of different moisture appear white in the photographs, while regions of more uniform high or low humidity appear black. Taylor's hypothesis has been used to convert from time-height graphs to vertical cross sections.

In Fig 5.8b for free convection, the "inverted U-shaped" tops of thermals shows up as white because they separate the dry FA air from the moister ML air. These structures are predominantly vertical. In Fig 5.8a for forced convection, the eddies are sheared into a much more horizontal or slanting orientation, with a much more chaotic appearance. Similar structures are apparent in the lidar-generated images shown in the frontispiece figure on page xiii, for (a) free and (b) forced convection.

5.2.5 Term V: Turbulent Transport

The quantity $\overline{w'e}$ represents the vertical turbulent flux of TKE. As for other vertical fluxes, the change in flux with height is more important than the magnitude of flux. Term V is a flux divergence term; if there is more flux into a layer than leaves, then the magnitude of TKE increases.

On a local scale (i.e., at any one height within the ML), Term V acts as either production or loss, depending on whether there is a flux convergence or divergence. When integrated over the depth of the ML, however, Term V becomes identically zero, assuming as bottom and top boundary conditions that the earth is not turbulent, and that there is negligible turbulence above the top of the ML. Overall, Term V neither creates nor destroys TKE, it just moves or redistributes TKE from one location in the BL to another.

Fig 5.9 shows vertical profiles of $\overline{w'e}$ for daytime, convective cases. Most of these

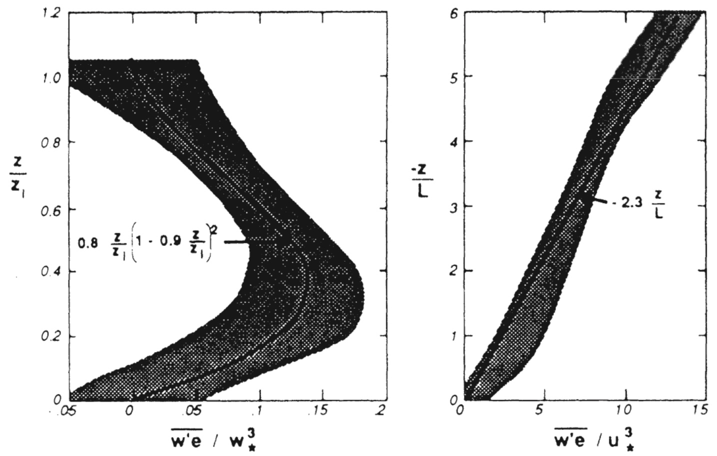

Fig. 5.9 Range of vertical profiles of the normalized vertical flux of turbulence kinetic energy using mixed layer scaling (left) and surface-layer scaling (right) where L is the Obukhov length. After Lenschow, et al. (1980), André, et al. (1978), Therry and Lacarrere (1983), and Pennell and LeMone (1974).

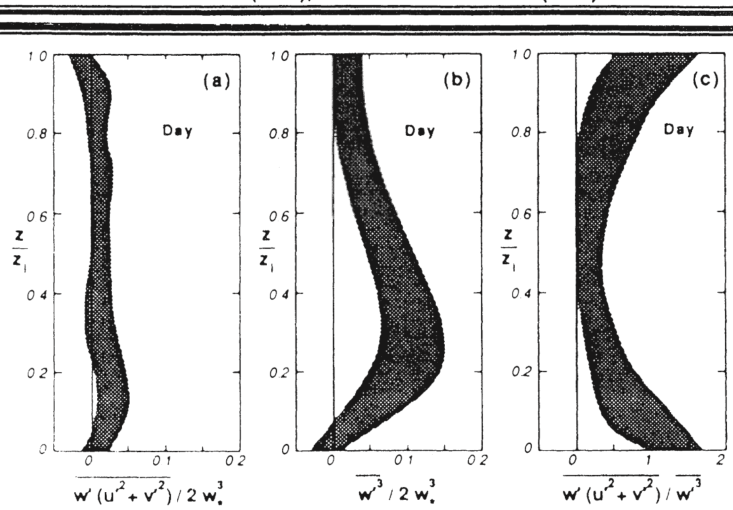

Fig. 5.10 (a) Range of vertical profiles of the normalized vertical flux of horizontal variance; (b), the vertical flux of vertical variance; (c), and the ratio of the two during daytime. After Lenschow, et al. (1980).

profiles show a maximum of $\overline{w'e}$ at $z/z_i = 0.3$ to 0.5 . Below this maximum, there is more upward flux leaving the top of any one layer than enters from below, making a net divergence or loss of TKE. Above the maximum, there is a net convergence or production of TKE. The net effect is that some of the TKE produced near the ground is transported up to the top half of the ML before it is dissipated, as confirmed in Fig 5.4. Transport across the surface layer is illustrated in the right portion of Fig 5.9, where the Obukhov length L will be defined in section 5.7.

If one splits the vertical turbulent transport of total TKE into transport of w'^2 and $(u'^2+v'^2)$, then one finds that it is the vertical transport of w'^2 that dominates in the middle of the ML, and the transport of $(u'^2+v'^2)$ that dominates near the surface. Fig 5.10 shows these transports, as well as their ratio.

5.2.6 Term VI: Pressure Correlation

Turbulence. Static pressure fluctuations are exceedingly difficult to measure in the atmosphere. The magnitudes of these fluctuations are very small, being on the order of 0.005 kPa (0.05 mb) in the convective surface layer to 0.001 kPa (0.01 mb) or less in the ML. Pressure sensors with sufficient sensitivity to measure these static pressure fluctuations are contaminated by the large dynamic pressure fluctuations associated with turbulent and mean motions. As a result, correlations such as $\overline{w'p'}$ calculated from experimental data often contain more noise than signal.

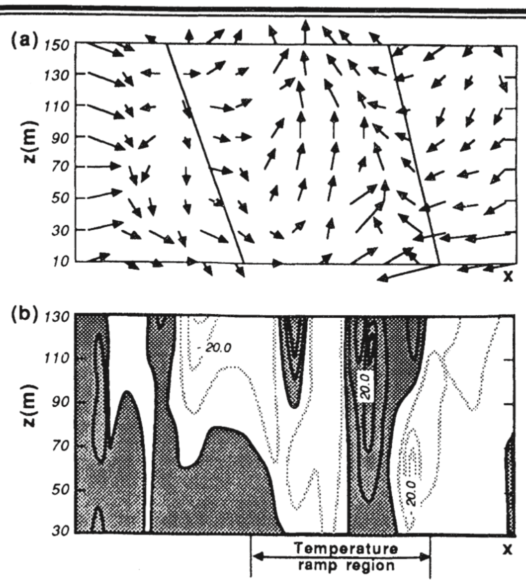

Fig. 5.11
(a) Composite of measured circulation patterns in a vertical cross-section thru convective thermals. Velocity vectors are deviations from the mean wind. Solid lines denote the boundaries of the temperature ramp associated with a thermal updraft; they are separated by a physical distance on the order of 100 m. (b) Contour x-z plot of $\overline{w'p'} / \rho u_*^3$, where the horizontal axis represents a composite of many thermals. Contour interval is 10.0. After Wilczak and Businger (1984).